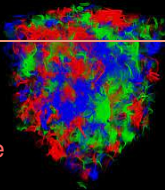




Lattice QCD with an inhomogeneous magnetic field background

XQCD 2022, Trondheim, Norway



Dean Valois

dvalois@physik.uni-bielefeld.de

Gergely Endrődi Bastian Brandt Gergely Marko Francesca Cuteri

July 27, 2022

Department of Physics
Bielefeld University

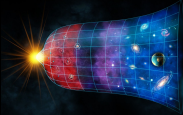
OUTLINE

1. Strongly magnetized physical systems
2. Magnetic field on the lattice
3. Lattice simulations
4. Summary & Conclusions

Strongly magnetized physical systems

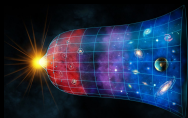
STRONGLY MAGNETIZED PHYSICAL SYSTEMS

Early universe
 $\rho \frac{eB}{eB} \quad 1.5 \text{ GeV}$

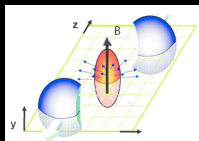


STRONGLY MAGNETIZED PHYSICAL SYSTEMS

Early universe
 $\rho \overline{eB}$ 1.5 GeV

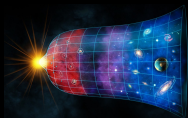


Heavy-ion collision
 $\rho \overline{eB}$ 0.5 GeV

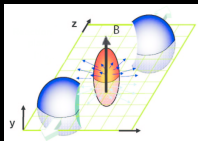


STRONGLY MAGNETIZED PHYSICAL SYSTEMS

Early universe
 $\rho \frac{eB}{eB}$ 1.5 GeV



Heavy-ion collision
 $\rho \frac{eB}{eB}$ 0.5 GeV

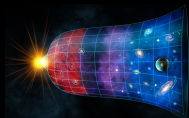


Neutron stars
 $\rho \frac{eB}{eB}$ 1 MeV

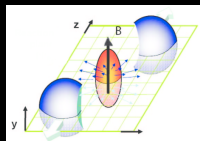


STRONGLY MAGNETIZED PHYSICAL SYSTEMS

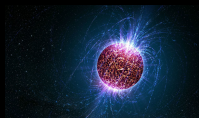
Early universe
 $\rho \frac{eB}{eB}$ 1.5 GeV



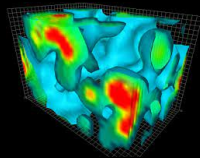
Heavy-ion collision
 $\rho \frac{eB}{eB}$ 0.5 GeV



Neutron stars
 $\rho \frac{eB}{eB}$ 1 MeV

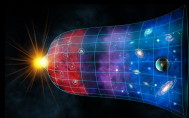


QCD vacuum

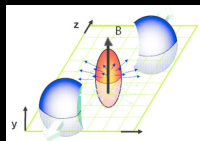


STRONGLY MAGNETIZED PHYSICAL SYSTEMS

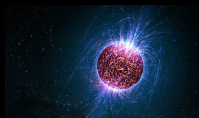
Early universe
 $\rho \overline{eB}$ 1.5 GeV



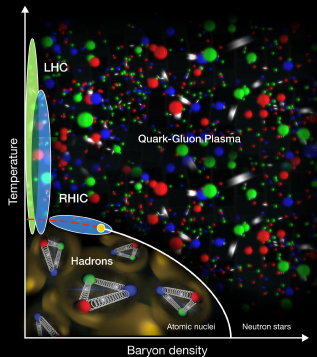
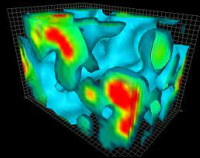
Heavy-ion collision
 $\rho \overline{eB}$ 0.5 GeV



Neutron stars
 $\rho \overline{eB}$ 1 MeV



QCD vacuum



MAGNETIC FIELDS IN HEAVY-ION COLLISIONS

MAGNETIC FIELDS IN HEAVY-ION COLLISIONS

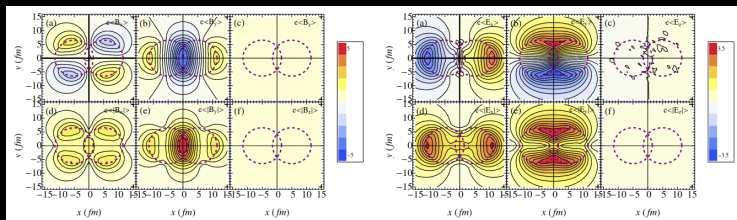



Figure 2: Spatial distributions of the electric (right) and magnetic (left) fields in the transverse plane for an impact parameter $b = 10$ fm  Deng and Huang 2012.

MAGNETIC FIELDS IN HEAVY-ION COLLISIONS

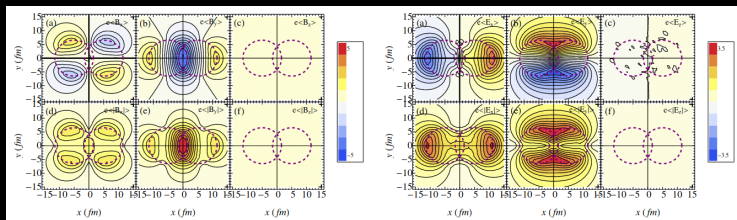



Figure 2: Spatial distributions of the electric (right) and magnetic (left) fields in the transverse plane for an impact parameter $b = 10$ fm  Deng and Huang 2012.

Caveats:

- \mathbf{B} and \mathbf{E} are highly non-homogeneous.

MAGNETIC FIELDS IN HEAVY-ION COLLISIONS

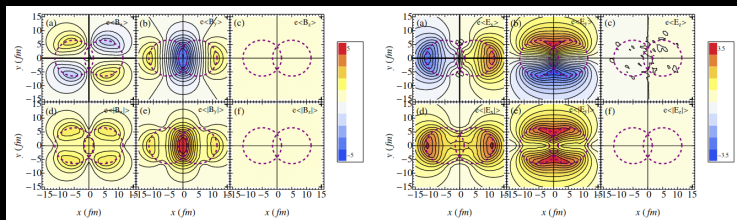



Figure 2: Spatial distributions of the electric (right) and magnetic (left) fields in the transverse plane for an impact parameter $b = 10$ fm  Deng and Huang 2012.

Caveats:

- \mathbf{B} and \mathbf{E} are highly non-homogeneous.
- A real \mathbf{E} leads to sign problem.

MAGNETIC FIELDS IN HEAVY-ION COLLISIONS

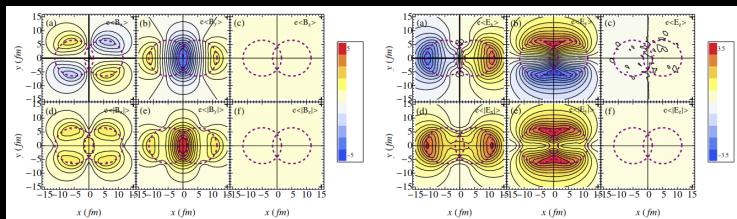



Figure 2: Spatial distributions of the electric (right) and magnetic (left) fields in the transverse plane for an impact parameter $b = 10$ fm  Deng and Huang 2012.

Caveats:

- \mathbf{B} and \mathbf{E} are highly non-homogeneous.
- A real \mathbf{E} leads to sign problem.
- No Minkowski time evolution from Euclidean simulations.

MAGNETIC FIELDS IN HEAVY-ION COLLISIONS

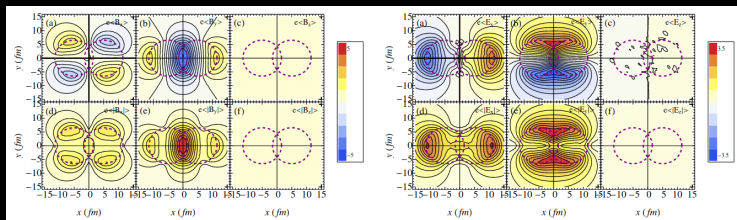



Figure 2: Spatial distributions of the electric (right) and magnetic (left) fields in the transverse plane for an impact parameter $b = 10$ fm  Deng and Huang 2012.

Caveats:

- \mathbf{B} and \mathbf{E} are highly non-homogeneous.
- A real \mathbf{E} leads to sign problem.
- No Minkowski time evolution from Euclidean simulations.

What can we do?

MAGNETIC FIELDS IN HEAVY-ION COLLISIONS

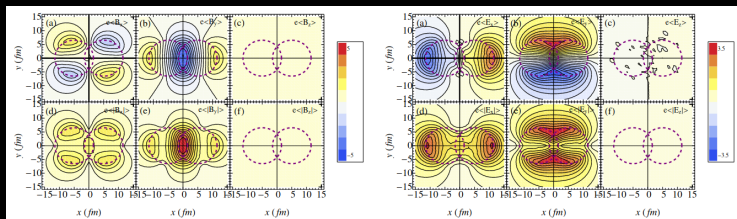


Figure 2: Spatial distributions of the electric (right) and magnetic (left) fields in the transverse plane for an impact parameter $b = 10$ fm [Deng and Huang 2012](#).

Caveats:

- \mathbf{B} and \mathbf{E} are highly non-homogeneous.
- A real \mathbf{E} leads to sign problem.
- No Minkowski time evolution from Euclidean simulations.

What can we do?

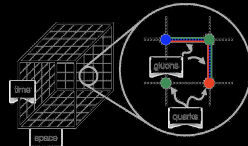
$B(x)$ as background in lattice QCD!

Magnetic field on the lattice

UNIFORM MAGNETIC FIELD ON THE LATTICE

fermion fields ψ ,
gluon fields $U = e^{iagA^b T_b} \in \text{SU}(3)$

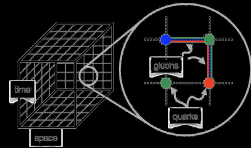
(anti-)periodic BC



UNIFORM MAGNETIC FIELD ON THE LATTICE

fermion fields ψ ,
 gluon fields $U = e^{iagA^b T_b} \in \text{SU}(3)$
 magnetic field $u = e^{iaqA} \in \text{U}(1)$

(anti-)periodic BC

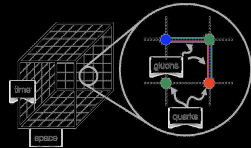


UNIFORM MAGNETIC FIELD ON THE LATTICE

fermion fields ψ ,
 gluon fields $U = e^{iagA^b T_b} \in \text{SU}(3)$
 magnetic field $u = e^{iaqA} \in \text{U}(1)$

$$\mathbf{B} = B\hat{z}$$

(anti-)periodic BC



UNIFORM MAGNETIC FIELD ON THE LATTICE

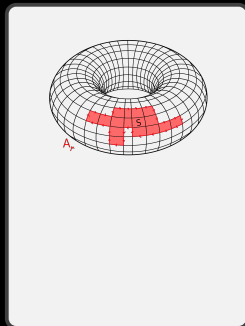
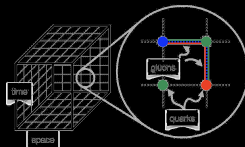
fermion fields ψ ,
 gluon fields $U = e^{iagA^b T_b} \in \text{SU}(3)$
 magnetic field $u = e^{iaqA} \in \text{U}(1)$

$$\mathbf{B} = B\hat{z}$$

Stoke's theorem must hold on the torus.

$$\text{inner area: } \int A dx = SB$$

(anti-)periodic BC



UNIFORM MAGNETIC FIELD ON THE LATTICE

fermion fields ψ
 gluon fields $U = e^{iagA^b T_b} \in \text{SU}(3)$
 magnetic field $u = e^{iaqA} \in \text{U}(1)$

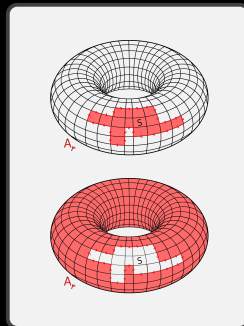
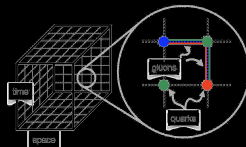
$$\mathbf{B} = B\hat{z}$$

Stoke's theorem must hold on the torus.

inner area: $A dx = SB$

outer area: $A dx = (L_x L_y - S)B$

(anti-)periodic BC



UNIFORM MAGNETIC FIELD ON THE LATTICE

fermion fields ψ ,
 gluon fields $U = e^{iagA^b T_b} \in \text{SU}(3)$
 magnetic field $u = e^{iaqA} \in \text{U}(1)$

$$\mathbf{B} = B\hat{z}$$

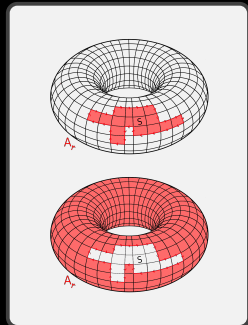
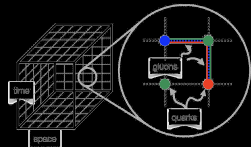
Stoke's theorem must hold on the torus.

inner area: $A dx = SB$

outer area: $A dx = (L_x L_y - S)B$

$$e^{iqBS} = e^{iqB(L_x L_y - S)}$$

(anti-)periodic BC



UNIFORM MAGNETIC FIELD ON THE LATTICE

fermion fields ! ,
 gluon fields ! $U = e^{iagA^b T_b} \in \text{SU}(3)$
 magnetic field ! $u = e^{iaqA} \in \text{U}(1)$

$$\mathbf{B} = B\hat{z}$$

Stoke's theorem must hold on the torus.

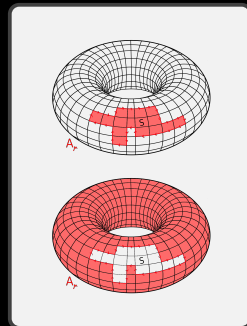
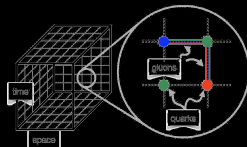
inner area: $A dx = SB$

outer area: $A dx = (L_x L_y - S)B$

$$e^{iqBS} = e^{iqB(L_x L_y - S)}$$

$$qB = \frac{2 N_b}{L_x L_y}; \quad N_b \in \mathbb{Z}$$

(anti-)periodic BC



UNIFORM MAGNETIC FIELD ON THE LATTICE

$$\mathbf{B} = r \quad \mathbf{A}$$

$$A_y = Bx \quad A_x = A_z = A_t = 0$$

UNIFORM MAGNETIC FIELD ON THE LATTICE

$$\mathbf{B} = r \quad \mathbf{A}$$

$$A_y = Bx \quad A_x = A_z = A_t = 0$$

$$u_y = e^{jaqBx} \quad u_x = u_z = u_t = 1$$

UNIFORM MAGNETIC FIELD ON THE LATTICE

$$\mathbf{B} = r \quad \mathbf{A}$$

$$A_y = Bx \quad A_x = A_z = A_t = 0$$

$$u_y = e^{iaqBx} \quad u_x = u_z = u_t = 1$$

$$u_y(L_x) = e^{ia2 Nb=L_y} \notin u_y(0)$$

UNIFORM MAGNETIC FIELD ON THE LATTICE

$$\mathbf{B} = r \quad \mathbf{A}$$

$$A_y = Bx \quad A_x = A_z = A_t = 0$$

$$u_y = e^{iaqBx} \quad u_x = u_z = u_t = 1$$

$$u_y(L_x) = e^{ia2 Nb=L_y} \notin u_y(0)$$

We can perform gauge transformations on the links

$$U^\rho(x) = (x)u \quad (x + a^\wedge)^y$$

a is the lattice spacing.

UNIFORM MAGNETIC FIELD ON THE LATTICE

$$\mathbf{B} = r \quad \mathbf{A}$$

$$A_y = Bx \quad A_x = A_z = A_t = 0$$

$$u_y = e^{jaqBx} \quad u_x = u_z = u_t = 1$$

$$u_y(L_x) = e^{ja2 Nb=L_y} \notin u_y(0)$$

We can perform gauge transformations on the links

$$u^\rho(x) = (x)u \quad (x + a^\wedge)^y$$

a is the lattice spacing.

$$u_x = \begin{cases} e^{iqBL_x y} & \text{if } x = L_x \quad a \\ 1 & \text{if } x \notin L_x \quad a \end{cases}$$

$$u_y = e^{jaqBx} \quad 0 \quad x \quad L_x \quad a$$



$$u_z = 1$$

$$u_t = 1$$

INHOMOGENEOUS MAGNETIC FIELD ON THE LATTICE



INHOMOGENEOUS MAGNETIC FIELD ON THE LATTICE

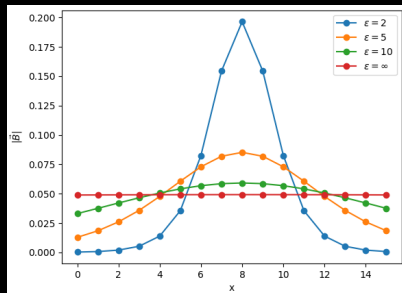
$$\mathbf{B} = \frac{B}{\cosh \frac{x}{L_x=2}} \hat{z}$$

Profile motivated by heavy-ion collision scenarios  Deng and Huang 2012,
 Cao 2018.

INHOMOGENEOUS MAGNETIC FIELD ON THE LATTICE

$$\mathbf{B} = \frac{B}{\cosh \frac{x}{L_x=2}} \hat{z}$$

Profile motivated by heavy-ion collision scenarios  Deng and Huang 2012,
 Cao 2018.

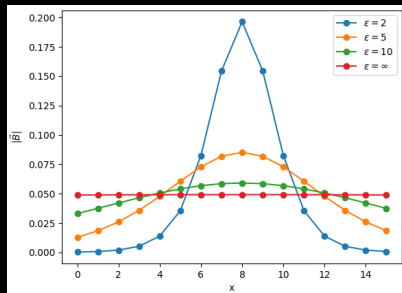


INHOMOGENEOUS MAGNETIC FIELD ON THE LATTICE

$$\mathbf{B} = \frac{B}{\cosh \frac{x - L_x/2}{2}} \hat{z}$$



Profile motivated by heavy-ion collision scenarios [Deng and Huang 2012](#),
[Cao 2018](#).

$$qB = \frac{N_b}{L_y \tanh \frac{L_x}{2}} \quad N_b \ll Z$$

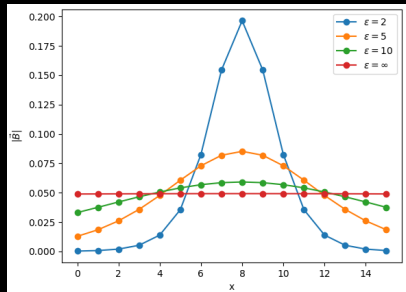


INHOMOGENEOUS MAGNETIC FIELD ON THE LATTICE

$$\mathbf{B} = \frac{B}{\cosh \frac{x - L_x/2}{2}} \hat{z}$$

Profile motivated by heavy-ion collision scenarios  Deng and Huang 2012,
 Cao 2018.

$$qB = \frac{N_b}{L_y \tanh \frac{L_x}{2}} \quad N_b \ll Z$$



$$u_x = \begin{cases} e^{2iqB y \tanh(\frac{L_x}{2})} & \text{if } x = L_x \\ 1 & \text{if } x \notin L_x \end{cases} \quad a$$

$$u_y = e^{iaqB [\tanh(\frac{x - L_x/2}{2}) + \tanh(\frac{L_x}{2})]}; \quad 0 \leq x \leq L_x \leq a$$

$$u_z = u_t = 1$$

Lattice simulations

THE SIMULATION SET UP

THE SIMULATION SET UP

- Improved staggered fermions with $N_f = 2 + 1$ flavors and physical masses;

THE SIMULATION SET UP

- Improved staggered fermions with $N_f = 2 + 1$ flavors and physical masses;
- Lattices: 16^3 6 24^3 8 28^3 10 36^3 12 !
continuum limit (lattice spacing $\neq 0$, $V = \text{const.}$);

THE SIMULATION SET UP

- Improved staggered fermions with $N_f = 2 + 1$ flavors and physical masses;
- Lattices: 16^3 6 24^3 8 28^3 10 36^3 12 a / continuum limit (lattice spacing $a \rightarrow 0$, $V = \text{const.}$);
- Number of gauge configurations $O(200) - O(700)$;

THE SIMULATION SET UP

- Improved staggered fermions with $N_f = 2 + 1$ flavors and physical masses;
- Lattices: $16^3 \times 6 \times 24^3 \times 8 \times 28^3 \times 10 \times 36^3 \times 12 \times \dots$ / continuum limit (lattice spacing $\neq 0$, $V = \text{const.}$);
- Number of gauge configurations $O(200) - O(700)$;
- Magnetic field

$$\mathbf{B} = \frac{B}{\cosh \frac{x}{L_x=2}} \hat{z} \quad eB = \frac{3 N_b}{L_y \tanh \frac{L_x}{2}} \quad 0.6 \text{ fm}$$

strength $0 \text{ GeV} \leq \frac{\rho}{eB} \leq 1.2 \text{ GeV}$;

THE SIMULATION SET UP

- Improved staggered fermions with $N_f = 2 + 1$ flavors and physical masses;
- Lattices: $16^3 \times 6 \times 24^3 \times 8 \times 28^3 \times 10 \times 36^3 \times 12 \times \dots$ / continuum limit (lattice spacing $\neq 0$, $V = \text{const.}$);
- Number of gauge configurations $\sim O(200) - O(700)$;
- Magnetic field

$$\mathbf{B} = \frac{B}{\cosh \frac{x}{L_x=2}} \hat{z} \quad eB = \frac{3 N_b}{L_y \tanh \frac{L_x}{2}} \quad 0.6 \text{ fm}$$

$$\text{strength } 0 \text{ GeV} \quad \rho_{eB} \quad 1.2 \text{ GeV};$$

- Temperature range $68 \text{ MeV} < T < 300 \text{ MeV}$ (crossover transition at $T_c = 155 \text{ MeV}$).

LATTICE OBSERVABLES

LATTICE OBSERVABLES

- Local chiral condensates (**u** and **d** quarks!)

LATTICE OBSERVABLES

- Local chiral condensates (**u** and **d** quarks!)

renormalization!

$$(x; T; B) = \frac{m_{ud}}{m^4} \quad (x; T; B) \quad (x; T; 0)$$

LATTICE OBSERVABLES

- Local chiral condensates (**u** and **d** quarks!)

$$\text{renormalization} \quad \langle \bar{\psi} \psi \rangle(x; T; B) = \frac{m_{ud}}{m^4} \langle \bar{\psi} \psi \rangle(x; T; B) \quad \langle \bar{\psi} \psi \rangle(x; T; 0)$$

- Local Polyakov loop

$$P = \frac{1}{L_x L_y} \sum_{y,z} \text{Re Tr} \prod_n U_t(x; y; z; n)$$

LATTICE OBSERVABLES

- Local chiral condensates (**u** and **d** quarks!)

$$\text{renormalization} \quad \langle \bar{\psi} \psi \rangle(x; T; B) = \frac{m_{ud}}{m^4} \langle \bar{\psi} \psi \rangle(x; T; B) \quad \langle \bar{\psi} \psi \rangle(x; T; 0)$$

- Local Polyakov loop

$$P = \frac{1}{L_x L_y} \sum_{y,z} \text{Re Tr}_n \prod U_t(x; y; z; n) \quad \text{renormalization} \quad \frac{P(x; T; B)}{P(x; T; 0)}$$

LATTICE OBSERVABLES

- Local chiral condensates (**u** and **d** quarks!)

$$\text{renormalization} \quad \langle \bar{\psi} \psi \rangle(x; T; B) = \frac{m_{ud}}{m^4} \langle \bar{\psi} \psi \rangle(x; T; B) \quad \langle \bar{\psi} \psi \rangle(x; T; 0)$$

- Local Polyakov loop

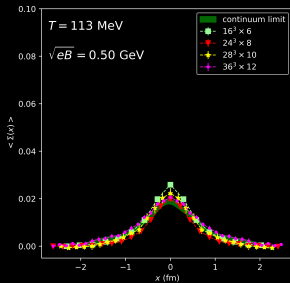
$$P = \frac{1}{L_x L_y} \sum_{y,z} \text{Re Tr} \prod_n U_t(x; y; z; n) \quad \text{renormalization} \quad \frac{P(x; T; B)}{P(x; T; 0)}$$

- Local electric currents (**u**, **d** and **s** quarks!)

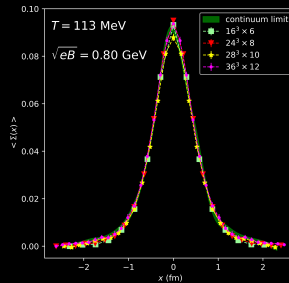
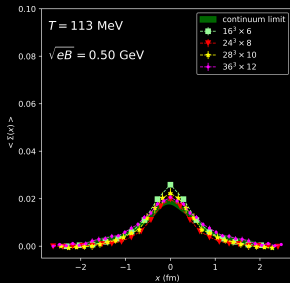
$$h J_i(x) = e \left(\frac{2}{3} u^i u^i - \frac{1}{3} d^i d^i - \frac{1}{3} s^i s^i \right)$$

$$\text{CHIRAL CONDENSATE} - (T; B) = \frac{m_{ud}}{m^4} [(T; B) \quad (T; 0)]$$

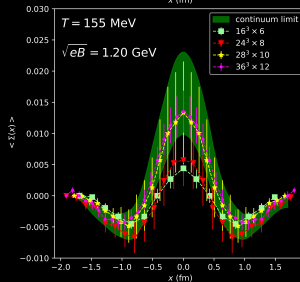
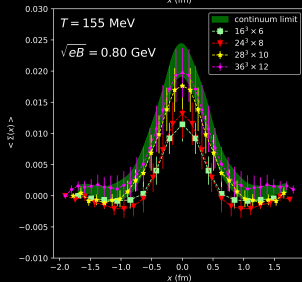
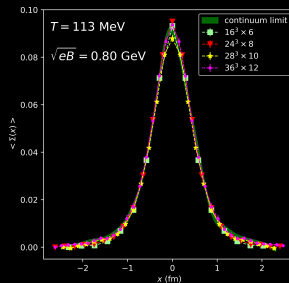
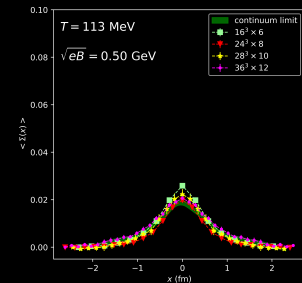
CHIRAL CONDENSATE - $(T; B) = \frac{m_{Ud}}{m^4} [(T; B) (T; 0)]$



CHIRAL CONDENSATE - $(T; B) = \frac{m_{Ud}}{m^4} [(T; B) (T; 0)]$



CHIRAL CONDENSATE - $(T; B) = \frac{m_{Ud}}{m^4} [(T; B) (T; 0)]$



CHIRAL CONDENSATE - $(T; B) = \frac{m_{ud}}{m^4} [(T; B) (T; 0)]$

What happens to the peak of the condensate as a function of T and B ?


$$\text{CHIRAL CONDENSATE} - \chi(T; B) = \frac{m_{ud}}{m^4} [\chi(T; B) - \chi(T; 0)]$$

What happens to the peak of the condensate as a function of T and B?

- Magnetic catalysis T away from T_c

$$\text{CHIRAL CONDENSATE} - \chi(T; B) = \frac{m_{ud}}{m^4} [\chi(T; B) - \chi(T; 0)]$$

What happens to the peak of the condensate as a function of T and B?

- Magnetic catalysis T away from T_c
- Inverse catalysis for T around T_c  Endrodi et al. 2019

POLYAKOV LOOP - $P(x; T; B) = P(x; T; 0)$

POLYAKOV LOOP - $P(x; T; B) = P(x; T; 0)$

POLYAKOV LOOP - $P(x; T; B) = P(x; T; 0)$

The Polyakov loop is typically broader than the chiral condensate.

POLYAKOV LOOP - $P(x; T; B) = P(x; T; 0)$

The Polyakov loop is typically broader than the chiral condensate.

$$\langle P(x) \rangle$$

$$\langle \chi(x) \rangle$$

POLYAKOV LOOP - $P(x; T; B) = P(x; T; 0)$

The Polyakov loop is typically broader than the chiral condensate.

$$\langle P(x) \rangle$$

$$\langle \chi(x) \rangle$$

The interaction of the condensate with P causes the dips!

ELECTRIC CURRENTS - $\mathbf{J}^i = \frac{1}{e} \sum_f q_f \mathbf{v}_f^i$

ELECTRIC CURRENTS - $\mathbf{J}^i = \frac{1}{e} \sum_f q_f \mathbf{v}_f^i$

$\mathbf{J} = \mathbf{r} \times \mathbf{B}$

ELECTRIC CURRENTS - $\mathbf{J}^i = \frac{1}{e} \sum_f q_f \mathbf{v}_f^i$

$$\mathbf{J} = \mathbf{r} \times \nabla \times \mathbf{B} = \nabla \times \mathbf{A}$$

ELECTRIC CURRENTS - $J^i = \frac{1}{P} \sum_f \frac{q_f}{e} v_f^i$

$$J_y = \frac{\partial B_z}{\partial x} = \frac{2B}{\cosh \frac{x}{L_x=2}} \tanh \frac{x}{L_x=2}$$

ELECTRIC CURRENTS - $J^i = \frac{1}{P} \sum_f \frac{q_f}{e} v_f^i$

$$J_y = \frac{\partial B_z}{\partial x} = \frac{2B}{\cosh \frac{x}{L_x=2}} \tanh \frac{x}{L_x=2}$$

ELECTRIC CURRENTS - $J^i = \frac{1}{e} \sum_f q_f v_f^i$

$$J_y = \frac{\partial B_z}{\partial x} = \frac{2B}{\cosh^2 \left(\frac{x}{L_x} \right)} \tanh \left(\frac{x}{L_x} \right)$$

Figure 6: Lattice electric currents for LHC-like ($\frac{p}{eB} = 0.5$ GeV) and RHIC-like ($\frac{p}{eB} = 0.1$ GeV) magnetic fields, respectively.

(BARE) MAGNETIC SUSCEPTIBILITY

(BARE) MAGNETIC SUSCEPTIBILITY

$$\frac{1}{\mu_0} \mathbf{B} = \mathbf{H} + \mathbf{M} \quad ! \quad \mathbf{J}_{\text{tot}} = \mathbf{J}_f + \mathbf{J}_m \quad ! \quad \mathbf{J}_m = \gamma \mathbf{M}$$

(BARE) MAGNETIC SUSCEPTIBILITY

$$\frac{1}{\mu_0} \mathbf{B} = \mathbf{H} + \mathbf{M} \quad ! \quad \mathbf{J}_{\text{tot}} = \mathbf{J}_f + \mathbf{J}_m \quad ! \quad \mathbf{J}_m = \gamma \mathbf{M}$$

- Linear medium:

$$\mathbf{M} = \chi_m \mathbf{H}$$

(BARE) MAGNETIC SUSCEPTIBILITY

$$\frac{1}{\mu_0} \mathbf{B} = \mathbf{H} + \mathbf{M} \quad ! \quad \mathbf{J}_{\text{tot}} = \mathbf{J}_f + \mathbf{J}_m \quad ! \quad \mathbf{J}_m = \gamma \mathbf{M}$$

- Linear medium:

$$\mathbf{M} = \chi_m \mathbf{H}$$

- $\frac{\chi_m}{1 + \chi_m} \gamma \mathbf{B} = \mathbf{J}_m$

(BARE) MAGNETIC SUSCEPTIBILITY

$$\frac{1}{\mu_0} \mathbf{B} = \mathbf{H} + \mathbf{M} \quad ! \quad \mathbf{J}_{\text{tot}} = \mathbf{J}_f + \mathbf{J}_m \quad ! \quad \mathbf{J}_m = \gamma \mathbf{M}$$

- Linear medium:

$$\mathbf{M} = \chi_m \mathbf{H}$$

- $\frac{\chi_m}{1 + \chi_m} \gamma \mathbf{B} = \mathbf{J}_m$

(BARE) MAGNETIC SUSCEPTIBILITY

$$\frac{1}{\mu_0} \mathbf{B} = \mathbf{H} + \mathbf{M} \quad ! \quad \mathbf{J}_{\text{tot}} = \mathbf{J}_f + \mathbf{J}_m \quad ! \quad \mathbf{J}_m = \gamma \mathbf{M}$$

- Linear medium:

$$\mathbf{M} = \chi_m \mathbf{H}$$

- $\frac{\chi_m}{1 + \chi_m} \gamma \mathbf{B} = \mathbf{J}_m$

(BARE) MAGNETIC SUSCEPTIBILITY

$$\frac{1}{\mu_0} \mathbf{B} = \mathbf{H} + \mathbf{M} \quad ! \quad \mathbf{J}_{\text{tot}} = \mathbf{J}_f + \mathbf{J}_m \quad ! \quad \mathbf{J}_m = \gamma \mathbf{M}$$

- Linear medium:

$$\mathbf{M} = \chi_m \mathbf{H}$$

- $\frac{\chi_m}{1 + \chi_m} \gamma \mathbf{M} = \mathbf{J}_m$

The susceptibility contains an additive
divergence $\chi_m \sim \log(a)$

(RENORMALIZED) MAGNETIC SUSCEPTIBILITY

The divergence is independent of T: $\chi_m(T) \sim \chi_m(0)$

(RENORMALIZED) MAGNETIC SUSCEPTIBILITY

The divergence is independent of T: $\chi_m(T) \sim \chi_m(0)$

(RENORMALIZED) MAGNETIC SUSCEPTIBILITY


The divergence is independent of T: $\chi_m(T) = \chi_m(0)$

- $\chi_m < 0$:
diamagnetism
- $\chi_m > 0$:
paramagnetism

(RENORMALIZED) MAGNETIC SUSCEPTIBILITY

The divergence is independent of T: $\chi_m(T) \sim \chi_m(0)$

- $\chi_m < 0$:
diamagnetism
- $\chi_m > 0$:
paramagnetism

Great agreement with the current-current method!  Bali, Gergely Endrodi,

and Piemonte 2020

Summary & Conclusions

SUMMARY & CONCLUSIONS

- A richer scenario emerges in the presence of an inhomogeneous B (dips, steady electric currents, etc.);

SUMMARY & CONCLUSIONS

- A richer scenario emerges in the presence of an inhomogeneous B (dips, steady electric currents, etc.);
- Electric currents are prominent for LHC-like magnetic fields and stronger;

SUMMARY & CONCLUSIONS

- A richer scenario emerges in the presence of an inhomogeneous B (dips, steady electric currents, etc.);
- Electric currents are prominent for LHC-like magnetic fields and stronger;
- Using J_m and Maxwell's equations we introduced a new method to compute χ_m ;

SUMMARY & CONCLUSIONS

- A richer scenario emerges in the presence of an inhomogeneous B (dips, steady electric currents, etc.);
- Electric currents are prominent for LHC-like magnetic fields and stronger;
- Using J_m and Maxwell's equations we introduced a new method to compute χ_m ;
- Our χ_m corroborates the picture of weak diamagnetism in QCD for $T < T_c$ and strong paramagnetism for $T > T_c$;

SUMMARY & CONCLUSIONS

- A richer scenario emerges in the presence of an inhomogeneous B (dips, steady electric currents, etc.);
- Electric currents are prominent for LHC-like magnetic fields and stronger;
- Using J_m and Maxwell's equations we introduced a new method to compute χ_m ;
- Our χ_m corroborates the picture of weak diamagnetism in QCD for $T < T_c$ and strong paramagnetism for $T > T_c$;
- The knowledge of these processes is important to capture the correct physics in heavy-ion collision studies (QCD models, hydrodynamics, etc.);

SUMMARY & CONCLUSIONS

- A richer scenario emerges in the presence of an inhomogeneous \mathbf{B} (dipoles, steady electric currents, etc.);
- Electric currents are prominent for LHC-like magnetic fields and stronger;
- Using \mathbf{J}_m and Maxwell's equations we introduced a new method to compute χ_m ;
- Our χ_m corroborates the picture of weak diamagnetism in QCD for $T < T_c$ and strong paramagnetism for $T > T_c$;
- The knowledge of these processes is important to capture the correct physics in heavy-ion collision studies (QCD models, hydrodynamics, etc.);

More on electromagnetic

- fields in lattice QCD:
posters by

BIBLIOGRAPHY I

References

Deng, Wei-Tian and Xu-Guang Huang (2012). “Event-by-event generation of electromagnetic fields in heavy-ion collisions”. In: *Physical Review C* 85.4, p. 044907.

Cao, Gaoqing (2018). “Chiral symmetry breaking in a semilocalized magnetic field”. In: *Physical Review D* 97.5, p. 054021.

Endrodi, G et al. (2019). “Magnetic catalysis and inverse catalysis for heavy pions”. In: *Journal of High Energy Physics* 2019.7, pp. 1–15.

BIBLIOGRAPHY II

- ▮ Bali, Gunnar S, Gergely Endrődi, and Stefano Piemonte (2020). “Magnetic susceptibility of QCD matter and its decomposition from the lattice”. In: *Journal of High Energy Physics* 2020.7, pp. 1–43.